High-Throughput Screening of Porous Crystalline Materials for Hydrogen Storage Capacity near Room Temperature

ARTICLE *in* THE JOURNAL OF PHYSICAL CHEMISTRY C · MARCH 2014

Impact Factor: 4.77 · DOI: 10.1021/jp4122326

4 AUTHORS, INCLUDING:

Yamil Javier Colón
University of Chicago
14 PUBLICATIONS **254** CITATIONS

SEE PROFILE

David Fairen-Jimenez
University of Cambridge
53 PUBLICATIONS **1,037** CITATIONS

SEE PROFILE

THE JOURNAL OF PHYSICAL CHEMISTRY C

Article

pubs.acs.org/JPCC

High-Throughput Screening of Porous Crystalline Materials for Hydrogen Storage Capacity near Room Temperature

Yamil J. Colón,[†] David Fairen-Jimenez,[†,‡] Christopher E. Wilmer,[§] and Randall Q. Snurr*

Department of Chemical and Biological Engineering, Northwestern University, 2145 Sheridan Road, Evanston, Illinois 60208, United States

Supporting Information

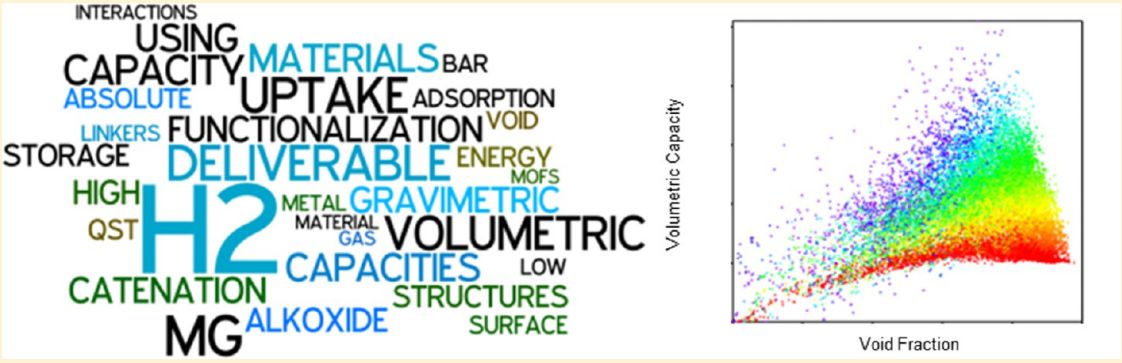

ABSTRACT: The hydrogen storage capabilities of 18 383 porous crystalline structures possessing various degrees of Mg functionalization and diverse physical properties were assessed through combined grand canonical Monte Carlo (GCMC) and quantum mechanical approaches. GCMC simulations were performed for pressures of 2 and 100 bar at a temperature of 243 K. Absolute uptake at 100 bar and deliverable capacity between 100 and 2 bar were calculated. Maximum absolute and deliverable gravimetric capacities were 9.35 and 9.12 wt %, respectively. Volumetrically, absolute and deliverable capacities were 51 and 30 g/L, respectively. The results reveal relationships between hydrogen uptake and the physical properties of the materials. We show that the introduction of an optimum amount of magnesium alkoxide to increase the isosteric heat of adsorption is a promising strategy to improve hydrogen uptake and delivery near ambient temperature.

INTRODUCTION

Hydrogen has long been proposed as a possible alternative to fossil fuels for powering vehicles.[1,2] It is particularly attractive because it is nontoxic and its oxidation product is water. However, hydrogen storage has proved challenging. The U.S. Department of Energy (DOE) has calculated that 4 kg or 44 000 L of gaseous H_2 is needed to provide enough energy to fuel a typical automobile.[3] This is translated to system requirements of 7.5 wt % and 70 g/L H_2 at a minimum temperature of 243 K and a maximum pressure of 100 bar.[4] The challenge is to design H_2 storage systems that efficiently and safely store H_2 in a realistic volume and that allow it to be easily extracted at reasonable pressures and temperatures. Several technologies are being developed to meet these goals, such as high-pressure gas and cryogenic tanks.[1,3] In addition, materials that chemisorb H_2, such as metal hydrides,[2,5] or physisorb H_2, such as metal–organic frameworks (MOFs),[6] are under intensive investigation.

In general, metal hydrides are capable of high uptake but bind hydrogen too tightly because the H_2 molecule is dissociated. The strong binding energy and slow H–H recombination kinetics make the release of hydrogen difficult. On the other hand, physisorption systems have the opposite problem: they bind H_2 too weakly, and although they are able to release it efficiently, their adsorption capacity is very limited, especially at room temperature.

MOFs are a widely studied class of H_2 storage materials.[7,8] They are porous, crystalline materials comprised of metal *nodes* connected by organic *linkers*. The great variety of possible nodes and linkers offers the opportunity to design and tune MOFs for particular applications. They possess large internal surface areas, up to 7100 m^2/g, which provide outstanding adsorption capacities.[9−12] Related materials, crystalline porous aromatic frameworks (PAFs), have also been reported recently.[13−15] PAFs have a diamond-like structure where tetrahedral carbon atoms act as nodes, linked by aromatic linkers. However, H_2 uptake in MOFs and PAFs at ambient temperature has thus far been low because the heats of adsorption have been too low. The highest experimental uptake values reported to date for room temperature hydrogen storage are ca. 2.3 wt % and 12.1 g/L (values refer to excess uptake).[7,8,16]

Received: December 13, 2013
Revised: February 19, 2014
Published: February 20, 2014

   dx.doi.org/10.1021/jp4122326 | J. Phys. Chem. C 2014, 118, 5383−5389

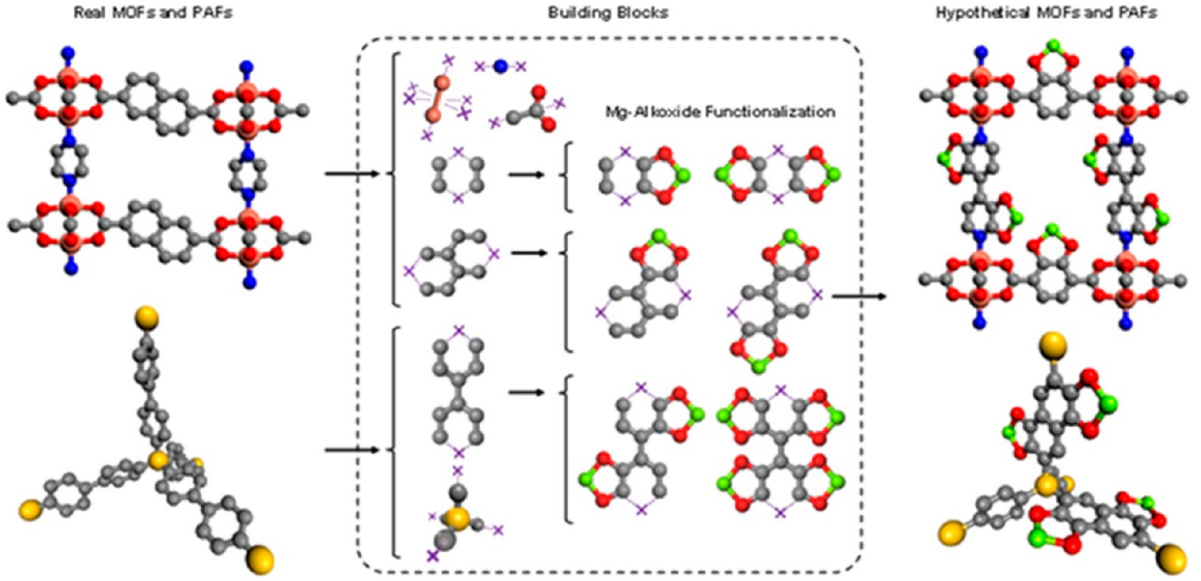

Figure 1. Our approach deconstructs known porous crystals into modular components (i.e., building blocks) that can be systematically reassembled into new, hypothetical materials. Before the building blocks are assembled into crystal structures, they can be functionalized to varying degrees with magnesium alkoxide groups. Hydrogen atoms have been omitted for clarity, and gray, red, pink, blue, yellow, and green spheres represent carbon, oxygen, copper, nitrogen, carbon node, and magnesium atoms, respectively. Purple "×" symbols represent sites where building blocks can be connected to each other.

Recently, metal alkoxide functionalization of the organic linkers through postsynthesis modification of hydroxyl protons has been demonstrated experimentally as a possibility to tune the surfaces of MOFs.[17,18] This approach has been shown to be promising for hydrogen storage because the positive charge of the metal interacts favorably with the H_2 quadrupole, increasing the capacity of the materials.[19−24] In preliminary work, we studied the interaction of various metal alkoxide groups (Li, Be, Mg, Mn, Fe, Ni, Cu, and Zn) with H_2 using MP2 and M06 quantum mechanical calculations.[24,25] Of these metals, we found magnesium to be best for H_2 storage and delivery, in agreement with other studies.[26,27] Magnesium alkoxide functional groups significantly improved storage capacities near room temperature in several structures relative to their unfunctionalized analogues. Magnesium's advantages, relative to other metals, are twofold. First, the H_2 binding energy is high, but not so high that it retains the H_2 at low pressure, which would reduce the deliverable capacity. Second, the H_2 binding energy is relatively constant as loading increases.

In this work, we aimed to determine whether there exists a plausible configuration of magnesium alkoxide functional groups in a porous material that would meet the DOE H_2 storage targets. Using recently developed structure-generating algorithms,[28] we created a library of 18 383 hypothetical structures with varying degrees of magnesium alkoxide functionalization and a diverse range of textural properties. Figure 1 illustrates how the structures were generated. The resulting materials were screened for H_2 uptake at 243 K at 2 and 100 bar using grand canonical Monte Carlo (GCMC) simulations, where the H_2 interactions with the magnesium alkoxide groups were modeled using ab initio quantum mechanical calculations.[24] From the GCMC simulations, we obtained the amount of H_2 adsorbed at 2 and 100 bar as well as the isosteric heats of adsorption (Q_{st}). The deliverable capacity was calculated by subtracting the amount of H_2 adsorbed at 2 bar from the amount adsorbed at 100 bar. From these data, gravimetric H_2 uptake and volumetric H_2 uptake (absolute and deliverable) were then related to various material properties.

METHODS

All 18 383 structures based on MOF and PAF precursors were generated using crystal enumeration algorithms previously reported.[28] The lists of nodes and linkers are provided in the Supporting Information. Figure 1 illustrates how the generation of the new structures takes place. Existing porous crystals are broken up into their building blocks. The organic linkers can then be functionalized to various degrees with magnesium alkoxides, providing new building blocks for the crystal generation. The metal or carbon nodes and linkers, described in Figures S2 and S3 (Supporting Information), are then combined to form new hypothetical crystals.

Interactions between H_2 molecules and the magnesium alkoxide functional groups were modeled using a Morse plus Coulomb potential. The potential was parametrized previously using quantum chemical calculations at the MP2/6-311+G** level of theory with counterpoise corrections to correct for basis set superposition errors (BSSEs).[24,29] Coulomb interactions were calculated using Ewald sums with partial charges on the alkoxide atoms[24] and the Darkrim−Levesque[30] model for H_2, which places charges of +0.468 on the H nuclei and a −0.936 charge on the center of mass.

H_2 interactions with all other framework atoms were described using Lennard-Jones (LJ) potentials, with parameters for the framework atoms taken from the universal force field (UFF).[31] H_2 LJ parameters were taken from the Michels−Degraaff−Tenseldam model.[32] H_2/H_2 interactions were modeled using an LJ + Coulomb potential using the LJ parameters from the Michels−Degraaff−Tenseldam model and charges from the Darkrim−Levesque model. All cross-terms were calculated using Lorentz−Berthelot mixing rules. A cutoff of 12.0 Å was used for the LJ interactions. All framework atoms

dx.doi.org/10.1021/jp4122326 | J. Phys. Chem. C 2014, 118, 5383−5389

were held fixed throughout the simulations, and the H_2 molecules were assumed to be rigid.

GCMC simulations were carried out using our in-house code RASPA.[33] Simulations were performed in cells with sufficient repeat units such that all edges were greater than 24 Å. In each simulation, 20 000 cycles were performed for system equilibration and another 20 000 were performed to calculate ensemble averages. In a cycle, an average of N moves were performed, where N is the number of molecules in the system. Monte Carlo moves were translation, rotation, insertion, deletion, and random reinsertion at a new position in the framework. Simulations were performed at pressures of 2 and 100 bar at a temperature of 243 K. Q_{st} was calculated from fluctuation theory during the GCMC simulation.[34]

Surface areas (SAs) were computed by rolling a N_2 probe of 3.681 Å over the framework atoms.[35] He void fractions for the structures were calculated using Widom insertions.[36]

RESULTS AND DISCUSSION

In a gas storage application, it is critical not only to obtain a high capacity at high pressure, but also to be able to release the adsorbed gas efficiently at lower pressure.[25,37] In a scenario where two structures have similar uptake at 100 bar but differing uptake at 2 bar (due to different adsorbent/adsorbate interaction strengths), the deliverable capacity of the structures will also be different. If the interactions are too strong, the structure will saturate at lower pressures, and this can harm the deliverable capacity. If they are too weak, the structure may not saturate even at 100 bar, but a higher deliverable capacity may be achieved. This is illustrated in Figure S1 (Supporting Information). Results in the literature indicate that, to improve hydrogen uptake in MOFs at 100 bar and near room temperature, it is necessary to increase the adsorbent/adsorbate interactions beyond what is observed in unfunctionalized MOFs.

While much work has focused on the gravimetric targets, in a typical automotive application, limited volume for the storage tank is the more critical problem, making the volumetric adsorption capacity particularly important. For the 18 383 structures generated, Figure 2 shows their ranking based on their H_2 volumetric deliverable capacities at ambient temperature (black). The deliverable gravimetric capacities are also shown in red. The maximum H_2 deliverable capacities obtained at 243 K are 30 g/L and 9.1 wt %. In general, those materials that excel in one uptake metric do not do as well in the other. For example, the material with the highest volumetric deliverable capacity (i.e., 30 g/L) falls short in the gravimetric capacity (i.e., 4.6 wt %). Furthermore, Figure 2 reveals that the materials among the top 3% in volumetric capacity show large differences in terms of gravimetric capacities, ranging from 2.5 to 6.0 wt %.

To analyze these differences, we studied the relationships between the H_2 storage capacities and the material properties. The structures generated show significant diversity and possess a wide range of structural characteristics. Generated structures range from 0 to 0.98 in helium void fraction, from 0 to 10 776 m^2/g in surface area, from 0 to 7.7 mmol/cm^3 in magnesium alkoxide density, and from 0 to 30.66 kJ/mol in isosteric heat of adsorption at 2 bar. Figure 3 and Figures S4 and S5 in the Supporting Information show the results obtained for absolute and deliverable H_2 uptake in both gravimetric and volumetric quantities. The gravimetric capacity increases with increasing void fraction, while the volumetric capacity has a maximum at

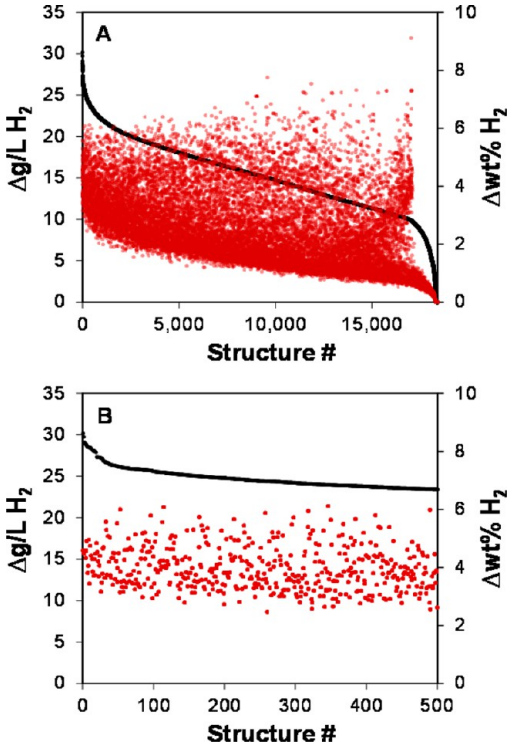

Figure 2. Ranking of MOF structures in terms of deliverable volumetric capacity (black points). Red points represent the corresponding deliverable gravimetric capacities. The lower panel shows the top 500 structures (i.e., top 3%) in volumetric capacity.

around 0.75 void fraction (Figure 3). There is a broad dispersion of capacities for any given void fraction. This is because the capacities depend not only on the void fraction, but also on multiple additional factors such as degree of functionalization and Q_{st}. The results show that the highest volumetric capacities are localized at 2.5 mmol/cm^3 magnesium alkoxide density and 17 kJ/mol Q_{st}. For gravimetric uptake, increasing Mg functionalization and higher Q_{st} increase the uptake at most void fractions (Figure 3). However, the materials with the very highest gravimetric uptake, surprisingly, have low Mg density and thus low Q_{st}. These materials have very high void fractions (>0.9), and there is a trade-off between the Mg density and the increase of loading of hydrogen molecules. In these open structures a significant amount of Mg is needed to improve the Mg density and hence the Q_{st}; however, this addition makes the material heavier, which is not beneficial from a gravimetric point of view. For both volumetric uptake and gravimetric uptake, Figures 3, S4, and S5 indicate a clear correlation between the degree of Mg functionalization and Q_{st}, which shows that magnesium alkoxide functionalization can be used to optimize the isosteric heat of adsorption and, in turn, H_2 uptake capacities.

The balance between gravimetric and volumetric deliverable capacities is explored in Figure 4. The structures with the highest gravimetric deliverable capacity, which are those with low Mg density, perform poorly in terms of the volumetric capacity. On the other hand, structures with high volumetric deliverable capacity (those with a Mg density of ca. 2.5 mmol/cm^3) have gravimetric deliverable capacities around 4 wt %, which is not bad, although it is less than the current targets. It is also interesting to note that structures with intermediate Mg densities possess intermediate volumetric deliverable capacities.

dx.doi.org/10.1021/jp4122326 | J. Phys. Chem. C 2014, 118, 5383−5389

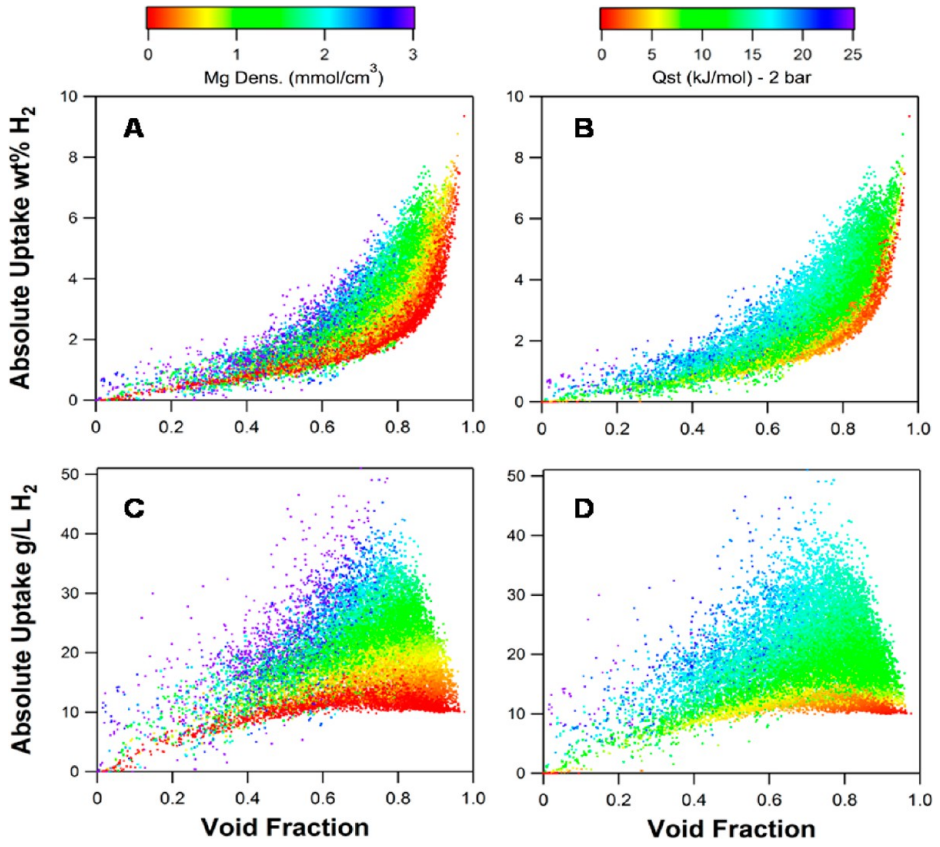

Figure 3. Absolute gravimetric (top) and volumetric (bottom) H_2 uptake versus void fraction obtained from simulated isotherms at 243 K and 100 bar on 18 383 different materials. Colors indicate the magnesium alkoxide density (left) and the isosteric heat of adsorption at 2 bar (right). Note that each point represents a single material. Alkoxide densities higher than 3 mmol/cm^3 are represented using the last color (i.e., purple).

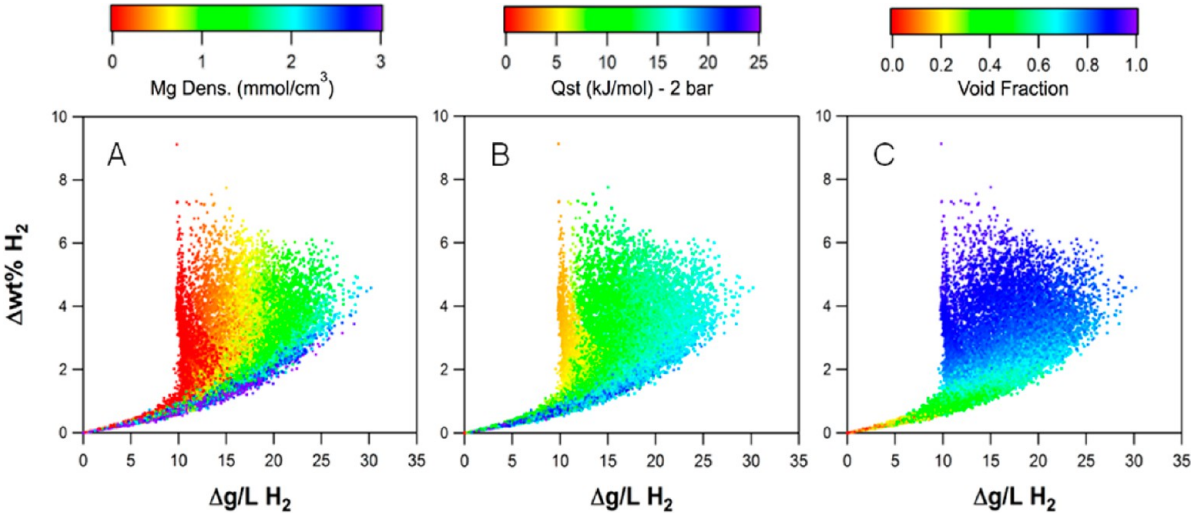

Figure 4. Deliverable gravimetric versus volumetric capacity obtained from simulated isotherms at 243 K and 2 and 100 bar. Colors indicate the magnesium alkoxide density (left), the isosteric heat of adsorption at 2 bar (center), and the void fraction (right).

There is a fundamental limitation that prevents a material from having large volumetric and gravimetric deliverable capacities simultaneously. For an optimal gravimetric capacity, the material should have a low framework density. The insertion of relatively heavy Mg metals compared with C, O, and H atoms does not improve this characteristic. On the other hand, for an optimal volumetric capacity there is a balance between void fraction and material density, confirming our previous findings, where the highest H_2 uptake corresponded to materials with not-so-high porosity.[38] In this case, the insertion of Mg metals only causes a small reduction in the pore volume that is compensated by the higher interaction and Q_{st}.

Although deliverable capacities are of critical importance for vehicular storage applications, the absolute capacities at a single pressure are related to the material characteristics in a more straightforward manner. Figure 5 shows the relation between absolute and deliverable capacities and the influence of Mg density (A, D), Q_{st} (B, E), and void fraction (C, F). To

dx.doi.org/10.1021/jp4122326 | J. Phys. Chem. C 2014, 118, 5383−5389

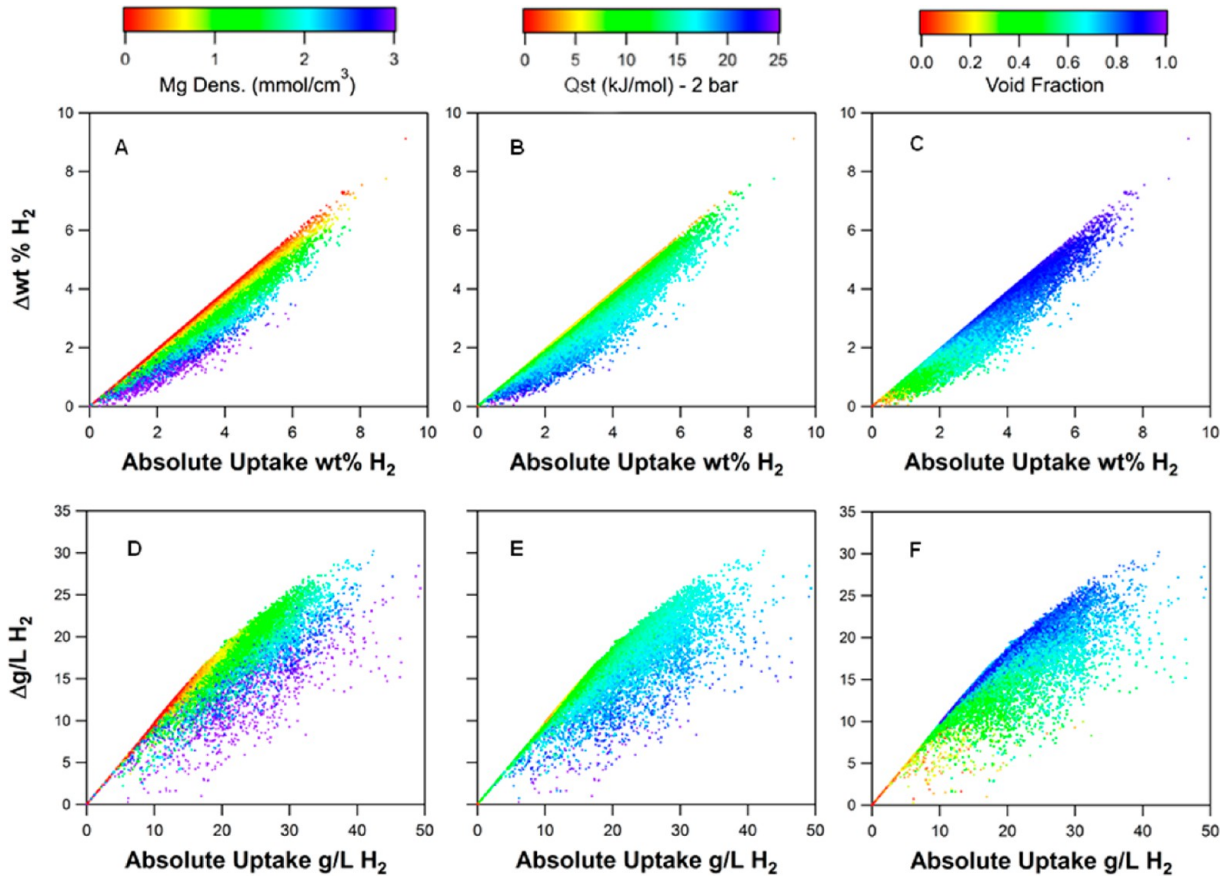

Figure 5. Deliverable capacity vs absolute uptake at 100 bar at 243 K, gravimetric (top) and volumetric (bottom). Colors indicate the magnesium alkoxide density (left), Q_{st} at 2 bar (center), and the void fraction (right).

maximize the absolute volumetric uptake at 100 bar, high values of Mg density (3 mmol/cm^3) and Q_{st} (ca. 25 kJ/mol) are necessary. However, as mentioned above, higher Q_{st} increases adsorption at low pressures, hence harming the deliverable capacity and causing the large differences between absolute and deliverable capacities observed in Figure 5. It is interesting to note that structures that possess optimum Mg densities and Q_{st} for gravimetric deliverable capacity (i.e., low Mg densities and Q_{st} values) show less difference between absolute and deliverable uptake, for both gravimetric and volumetric capacities. For example, the best gravimetric structure shows 9.35 wt % absolute vs 9.12 wt % deliverable capacity with 0.0 mmol/cm^3 and 3.2 kJ/mol values of Mg density and Q_{st}, respectively. In the case of volumetric capacity, there are only small differences between absolute and deliverable capacities up to ca. 17 g/L (absolute) for Mg density and Q_{st} values of ca. 0.0 mmol/cm^3 and 6 kJ/mol, respectively.

Figure 5 also reveals that the structures with the highest void fractions deviate to a lesser degree when comparing the absolute and deliverable amounts despite high Mg functionalization and, consequently, high Q_{st}. With a high void fraction not only the absolute but also the deliverable quantities may be increased.

To obtain MOFs and PAFs with large pore volumes and surface areas, one can increase the length of the organic linkers. However, this increases the possibility of catenation.[39] Network catenation occurs when two or more independent, identical networks are entangled, partially filling each other's pores. Catenation results in a decrease of the void fraction and the pore volume. Figure 6 and Figure S6 in the Supporting Information show the influence of catenation on the absolute uptake as a function of the volumetric and gravimetric surface area, respectively. Figure S7 (Supporting Information) shows the influence of catenation on deliverable uptake as a function of the void fraction. The gravimetric uptake (Figure 6, top) reveals two distinct regions composed of different types of materials. The materials comprising the upper region with a negative slope are those which have the possibility to be catenated due to their high pore volume, but are not. The materials in the lower region with a positive slope are the catenated materials or those that due to their low porosity do not have this possibility. Figure 6 shows that the different uptake values observed within each region are a consequence of the Mg functionalization. Within one region, and for similar volumetric surface areas, materials with higher Mg density show higher absolute uptake. This result suggests a path for optimizing future H_2 storage materials. Namely, through the development of new synthetic techniques to prevent catenation in structures that otherwise would be catenated, higher absolute uptake capacities may be achieved.

For absolute volumetric uptake (Figure 6, lower panels), the catenation effect is not as clear, but the effect of Mg density is evident. Interestingly, the apparent slope of each region increases with Mg functionalization. Plotting absolute uptake (gravimetric and volumetric) versus gravimetric surface area reveals trends similar to those observed for volumetric uptake versus volumetric surface area (Figure S6, Supporting Information).

dx.doi.org/10.1021/jp4122326 | J. Phys. Chem. C 2014, 118, 5383−5389

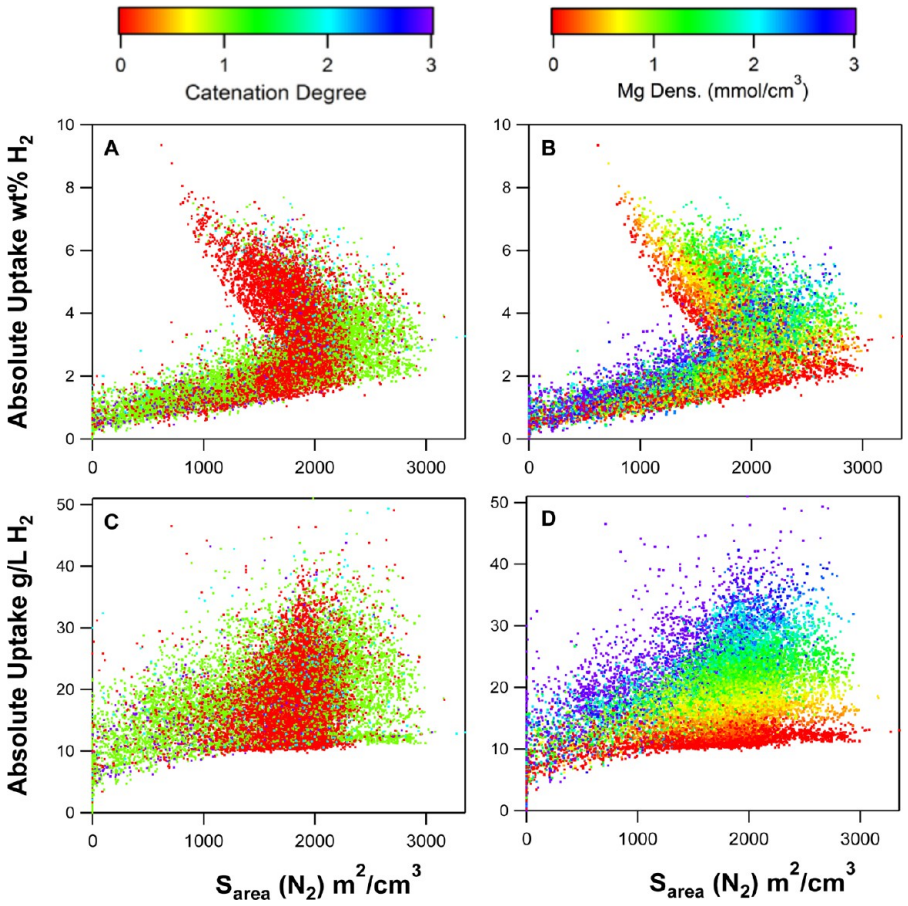

Figure 6. Gravimetric and volumetric H_2 absolute uptake at 100 bar and 243 K as a function of the volumetric surface area. Colors indicate the catenation degree (left) and magnesium alkoxide density (right).

CONCLUSIONS

In this work, we screened 18 383 new hypothetical structures with varying degrees of magnesium alkoxide functionalization for possible H_2 storage applications and revealed important structure/property relationships. For optimizing deliverable gravimetric hydrogen uptake at 243 K in porous materials, our calculations suggest very high void fractions (>0.9) and low Mg density (0.0−0.5 mmol/cm^3). To optimize deliverable volumetric hydrogen uptake at 243 K, our simulations suggest a void fraction of 0.75 and Mg density of 2.5 mmol/cm^3. Large-scale, high-throughput computational screening of the adsorption properties of materials allows us to explore what could be the ultimate limits of these types of porous media.

ASSOCIATED CONTENT

Supporting Information

Description of the hydrogen deliverable capacity, structures of the nodes and linkers used in MOF generation, functionalization of the linkers, additional structure/property results, representative high-performing structures, and a figure showing the absolute gravimetric H_2 uptake versus pressure obtained for UFF vs Dreiding force fields. This material is available free of charge via the Internet at http://pubs.acs.org.

AUTHOR INFORMATION

Corresponding Author

*E-mail: snurr@northwestern.edu.

Present Addresses

‡D.F.-J.: Department of Chemical Engineering and Biotechnology, University of Cambridge, Pembroke St., Cambridge CB2 3RA, U.K.

§C.E.W.: Department of Chemical and Petroleum Engineering, University of Pittsburgh, 3700 O'Hara St., Pittsburgh, PA 15261, U.S.A. (starting September 2014).

Author Contributions

†Y.J.C. and D.F.-J. contributed equally to this work.

Notes

The authors declare the following competing financial interest(s): C.E.W. and R.Q.S. have a financial interest in the startup company NuMat Technologies, which is seeking to commercialize metal−organic frameworks..

ACKNOWLEDGMENTS

This research was supported by the U.S. Department of Energy (Grant DE-FG02-08ER15967). This material is based upon work supported by the National Science Foundation Graduate Research Fellowship under Grant DGE-0824162 (Y.J.C.). D.F.-J. acknowledges the Royal Society (United Kingdom) for a University Research Fellowship. We gratefully acknowledge Northwestern University's Quest cluster and the National Energy Research Scientific Computing Center's Carver Cluster for computer resources.

REFERENCES

(1) Jorgensen, S. W. Hydrogen Storage Tanks for Vehicles: Recent Progress and Current Status. *Curr. Opin. Solid State Mater. Sci.* **2011**, *15*, 39−43.

(2) David, W. I. F. Effective Hydrogen Storage: A Strategic Chemistry Challenge. *Faraday Discuss.* **2011**, *151*, 399−414.

(3) U.S. Department of Energy. Energy Efficiency and Renewable Energy. http://www1.eere.energy.gov/hydrogenandfuelcells/storage/current_technology.html (accessed March 2013).

(4) U.S. Department of Energy. DOE Targets for Onboard Hydrogen Storage Systems for Light-Duty Vehicles. http://www1.eere.energy.gov/hydrogenandfuelcells/storage/pdfs/targets_onboard_hydro_storage.pdf (accessed March 2013).

(5) Sakintuna, B.; Darkrim, F. L.; Hischer, M. Metal Hydride Materials for Solid Hydrogen Storage: A Review. *Int. J. Hydrogen Energy* **2007**, *32*, 1121−1140.

(6) Rowsell, J. L. C.; Yaghi, O. M. Strategies for Hydrogen Storage in Metal−Organic Frameworks. *Angew. Chem., Int. Ed.* **2005**, *44*, 4670−4679.

(7) Murray, L. J.; Dinca, M.; Long, J. R. Hydrogen Storage in Metal−Organic Frameworks. *Chem. Soc. Rev.* **2009**, *38*, 1294−1314.

(8) Suh, M. P.; Park, H. J.; Prasad, T. K.; Lim, D.-W. Hydrogen Storage in Metal−Organic Frameworks. *Chem. Rev.* **2011**, *112*, 782−835.

(9) Farha, O. K.; Yazaydin, A. O.; Eryazici, I.; Malliakas, C. D.; Hauser, B. G.; Kanatzidis, M. G.; Nguyen, S. T.; Snurr, R. Q.; Hupp, J. T. De Novo Synthesis of a Metal−Organic Framework Material Featuring Ultrahigh Surface Area and Gas Storage Capacities. *Nat. Chem.* **2010**, *2*, 944−948.

(10) Farha, O. K.; Eryazici, I.; Jeong, N. C.; Hauser, B. G.; Wilmer, C. E.; Sarjeant, A. A.; Snurr, R. Q.; Nguyen, S. T.; Yazaydın, A. Ö.; Hupp, J. T. Metal−Organic Framework Materials with Ultrahigh Surface Areas: Is the Sky the Limit? *J. Am. Chem. Soc.* **2012**, *134*, 15016−15021.

(11) Furukawa, H.; Ko, N.; Go, Y. B.; Aratani, N.; Choi, S. B.; Choi, E.; Yazaydin, A. O.; Snurr, R. Q.; O'Keeffe, M.; Kim, J.; et al. Ultrahigh Porosity in Metal−Organic Frameworks. *Science* **2010**, *329*, 424−428.

(12) Sarkisov, L. Accessible Surface Area of Porous Materials: Understanding Theoretical Limits. *Adv. Mater.* **2012**, *24*, 3130−3133.

(13) Ben, T.; Ren, H.; Ma, S.; Cao, D.; Lan, J.; Jing, X.; Wang, W.; Xu, J.; Deng, F.; Simmons, J. M.; et al. Targeted Synthesis of a Porous Aromatic Framework with High Stability and Exceptionally High Surface Area. *Angew. Chem., Int. Ed.* **2009**, *48*, 9457−9460.

(14) Lan, J.; Cao, D.; Wang, W.; Ben, T.; Zhu, G. High-Capacity Hydrogen Storage in Porous Aromatic Frameworks with Diamond-like Structure. *J. Phys. Chem. Lett.* **2010**, *1*, 978−981.

(15) Ben, T.; Pei, C.; Zhang, D.; Xu, J.; Deng, F.; Jing, X.; Qiu, S. Gas Storage in Porous Aromatic Frameworks (PAFs). *Energy Environ. Sci.* **2011**, *4*, 3991−3999.

(16) Lim, W.-X.; Thornton, A. W.; Hill, A. J.; Cox, B. J.; Hill, J. M.; Hill, M. R. High Performance Hydrogen Storage from Be-BTB Metal−Organic Framework at Room Temperature. *Langmuir* **2013**, *29*, 8524−8533.

(17) Mulfort, K. L.; Farha, O. K.; Stern, C. L.; Sarjeant, A. A.; Hupp, J. T. Post-Synthesis Alkoxide Formation within Metal−Organic Framework Materials: A Strategy for Incorporating Highly Coordinatively Unsaturated Metal Ions. *J. Am. Chem. Soc.* **2009**, *131*, 3866−3868.

(18) Himsl, D.; Wallacher, D.; Hartmann, M. Improving the Hydrogen-Adsorption Properties of a Hydroxy-Modified MIL-53(Al) Structural Analogue by Lithium Doping. *Angew. Chem., Int. Ed.* **2009**, *48*, 4639−4642.

(19) Lochan, R. C.; Head-Gordon, M. Computational Studies of Molecular Hydrogen Binding Affinities: The Role of Dispersion Forces, Electrostatics, and Orbital Interactions. *Phys. Chem. Chem. Phys.* **2006**, *8*, 1357−1370.

(20) Yang, Q. Y.; Zhong, C. L. Understanding Hydrogen Adsorption in Metal−Organic Frameworks with Open Metal Sites: A Computational Study. *J. Phys. Chem. B Lett.* **2006**, *110*, 655−658.

(21) Sun, Y. Y.; Kim, Y.-H.; Zhang, S. B. Effect of Spin State on the Dihydrogen Binding Strength to Transition Metal Centers in Metal−Organic Frameworks. *J. Am. Chem. Soc.* **2007**, *129*, 12606−12607.

(22) Lochan, R. C.; Khaliullin, R. Z.; Head-Gordon, M. Interaction of Molecular Hydrogen with Open Transition Metal Centers for Enhanced Binding in Metal−Organic Frameworks: A Computational Study. *Inorg. Chem.* **2008**, *47*, 4032−4044.

(23) Dinca, M.; Long, J. R. Hydrogen Storage in Microporous Metal−Organic Frameworks with Exposed Metal Sites. *Angew. Chem., Int. Ed.* **2008**, *47*, 6766−6779.

(24) Getman, R. B.; Miller, J. H.; Wang, K.; Snurr, R. Q. Metal Alkoxide Functionalization in Metal−Organic Frameworks for Enhanced Ambient Temperature Hydrogen Storage. *J. Phys. Chem. C* **2011**, *115*, 2066−2075.

(25) Brand, S. K.; Colón, Y. J.; Getman, R. B.; Snurr, R. Q. Design Strategies for Metal Alkoxide Functionalized Metal−Organic Frameworks for Ambient Temperature Hydrogen Storage. *Microporous Mesoporous Mater.* **2013**, *171*, 103−109.

(26) Tylianakis, E.; Klontzas, E.; Froudakis, G. E. The Effect of Structural and Energetic Parameters of MOFs and COFs towards the Improvement of Their Hydrogen Storage Properties. *Nanotechnology* **2009**, *20*, 204030.

(27) Stergiannakos, T.; Tylianakis, E.; Klontzas, E.; Froudakis, G. E. Enhancement of Hydrogen Adsorption in Metal−Organic Frameworks by Mg^{2+} Functionalization: A Multiscale Computational Study. *J. Phys. Chem. C* **2010**, *114*, 16855−16858.

(28) Wilmer, C. E.; Leaf, M.; Lee, C. Y.; Farha, O. K.; Hauser, B. G.; Hupp, J. T.; Snurr, R. Q. Large-Scale Screening of Hypothetical Metal−Organic Frameworks. *Nat. Chem.* **2012**, 83−89.

(29) Boys, S. F.; Bernardi, F. The Calculation of Small Molecular Interactions by the Differences of Separate Total Energies. Some Procedures with Reduced Errors. *Mol. Phys.* **2002**, *100*, 65−73.

(30) Darkrim, F.; Levesque, D. Monte Carlo Simulations of Hydrogen Adsorption in Single-Walled Carbon Nanotubes. *J. Chem. Phys.* **1998**, *109*, 4981−4984.

(31) Rappé, A. K.; Casewit, C. J.; Colwell, K. S.; Goddard, W. A., III; Skiff, W. M. UFF, a Full Periodic Table Force Field for Molecular Mechanics and Molecular Dynamics Simulations. *J. Am. Chem. Soc.* **1992**, *114*, 10024−10035.

(32) Michels, A.; Degraaff, W.; Tenseldam, C. A. Virial Coefficients of Hydrogen and Deuterium at Temperatures between −175 °C and +150 °C—Conclusions from the 2nd Virial Coefficient with Regards to the Intermolecular Potential. *Physica* **1960**, *26*, 393−408.

(33) Dubbeldam, D.; Calero, S.; Ellis, D. E.; Snurr, R. Q. *RASPA*, version 1.0; Northwestern University: Evanston, IL, 2008.

(34) Karavias, F.; Myers, A. L. Isosteric Heats of Multicomponent Adsorption: Thermodynamics and Computer Simulations. *Langmuir* **1991**, *7*, 3118−3126.

(35) Düren, T.; Bae, Y.-S.; Snurr, R. Q. Using Molecular Simulation to Characterise Metal−Organic Frameworks for Adsorption Applications. *Chem. Soc. Rev.* **2009**, *38*, 1237−1247.

(36) Myers, A. L.; Monson, P. A. Adsorption in Porous Materials at High Pressure: Theory and Experiment. *Langmuir* **2002**, *18*, 10261−10273.

(37) Bae, Y.-S.; Snurr, R. Q. Optimal Isosteric Heat of Adsorption for Hydrogen Storage and Delivery Using Metal−Organic Frameworks. *Microporous Mesoporous Mater.* **2010**, *132*, 300−303.

(38) Fairen-Jimenez, D.; Colón, Y. J.; Farha, O. K.; Bae, Y.-S.; Hupp, J. T.; Snurr, R. Q. Understanding Excess Uptake Maxima for Hydrogen Adsorption Isotherms in Frameworks with *rht* Topology. *Chem. Commun.* **2012**, *48*, 10496−10498.

(39) Rosi, N. L.; Eddaoudi, M.; Kim, J.; O'Keeffe, M.; Yaghi, O. M. Infinite Secondary Building Units and Forbidden Catenation in Metal−Organic Frameworks. *Angew. Chem., Int. Ed.* **2002**, *41*, 284−287.